

Coincidental emission of molecular ions from keV carbon cluster impacts

J.E. Locklear, S.V. Verkhoturov, E.A. Schweikert*

Department of Chemistry, Texas A&M University, College Station, Texas 77842-3012, TX, USA

Received 25 June 2004; accepted 5 August 2004

Available online 18 September 2004

Abstract

We report here experimental data for the emission of one and two phenylalanine (Ph) molecular ions per impact from 10 to 21 keV impacts of coronene ($C_{24}H_{12}$), C_{60} , and gramicidin S ($C_{60}N_{12}O_{10}H_{92}$) projectiles as a function of projectile mass, energy, and geometry. Secondary ion mass spectrometry (SIMS) experiments were conducted using event-by-event bombardment and detection. With this method, individual projectile impacts and the resulting secondary ions are recognized as singular events resolved in time and space. The target surface was an equa-molar mixture of phenylalanine (Ph_H , $C_9H_{11}NO_2$) and deuterated phenylalanine (Ph_D , $C_9H_3D_8NO_2$). This allowed for the detection of two co-emitted $[M-H]^-$ phenylalanine ions in a dual time-of-flight instrument. In contrast to the linear dependence yield of Ph versus energy for single Ph ion emission, the yield for two Ph ion emission versus energy is nonlinear within the experimental energy range. For the co-emission of two Ph ions, C_{60} was found to be more efficient than coronene at equal velocities.

© 2004 Elsevier B.V. All rights reserved.

Keywords: Secondary ion emission; Multi-ion emission; C_{60} ; Polyatomic projectiles; Cluster projectiles

1. Introduction

A number of studies have shown a ‘cluster effect’, i.e., increased secondary ion yields when a surface is bombarded with keV polyatomic projectiles at equal velocities [1–10]. The secondary emissions produced by these keV projectiles are not all equivalent. Most impacts result in the detection of no secondary ions. However, there are some impacts that produce multiple secondary ions. A study conducted with gold clusters examined the co-emission of two molecular ions as a function of projectile characteristics. The study found enhancement in secondary ion yields and the yields of two co-emitted molecular ions from individual events by atomic and polyatomic gold clusters [2]. Studies have shown 1–3 orders of magnitude increases in secondary ion yields with C_{60} compared to atomic projectiles at equal velocities [4] and have also observed low damage cross sections for C_{60} [9,11]. Since these properties have been demonstrated with C_{60} , it is of interest to investigate multi-ion emission produced by C_{60} .

In addition to C_{60} , two other carbon containing molecules (coronene and gramicidin S) were also used to investigate multi-ion emission as a function of projectile characteristics. We report here the first experimental data for the co-emission of two phenylalanine (Ph) molecular ions from keV coronene ($C_{24}H_{12}$), C_{60} , and gramicidin S ($C_{60}N_{12}O_{10}H_{92}$) projectile impacts as a function of projectile characteristics.

This study was conducted using event-by-event bombardment and detection described in detail elsewhere [4]. With this method, individual projectile impacts and the resulting secondary ions are recognized as singular events resolved in time and space. The results of multiple impacts are summed to produce analytically significant data.

It has been demonstrated that non-imaging characterization of nano-volumes is possible using the event-by-event technique [12]. Secondary ion (SI) emission is thought to originate from a volume about 10 nm in diameter. Since ejected secondary ions originate from this region, the ions must have a spatial relationship within the desorption volume. Observing co-emitted ions originating from individual ion impacts renders spatial relationships of specific species on the surface. The effectiveness of the nano-characterization de-

* Corresponding author. Tel.: +1 979 845 2341; fax: +1 979 845 1655.

E-mail address: schweikert@mail.chem.tamu.edu (E.A. Schweikert).

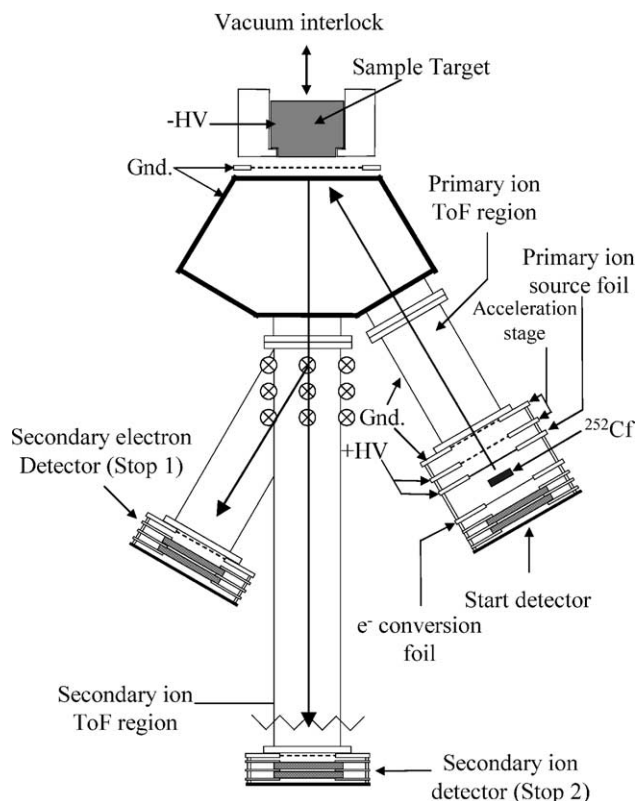


Fig. 1. Schematic diagram of the carbon cluster time-of-flight mass spectrometer.

depends on the occurrence of multi-ion events. Therefore, projectiles that produce more analytically significant multi-ion emissions would increase the effectiveness of non-imaging nano-characterization [12].

2. Experimental

2.1. Instrumental

A dual time-of-flight (ToF) instrument was used in this experiment (Fig. 1). Primary ions (PIs) are produced from a sputtering source using ^{252}Cf fission fragments. Approximately three percent of the activity of ^{252}Cf produces MeV fission fragments (FF) that are emitted about 180° from each other. One fission fragment starts the timing electronics by passing through a negatively biased conversion foil which produces electrons that impact a microchannel plate (MCP) assembly. The complementary fragment causes desorption/ionization of a source material coating an aluminized mylar foil. The desorbed ions are used as PIs for SIMS. The PIs are accelerated in two steps up to a maximum of 21 keV. First, 3.5–14.5 keV primary ions separate in a 14 cm primary ToF region. The positively charged PIs are accelerated a second time as they approach a sample target biased at -6.5 kV at 30° from normal. Once a primary ion (PI) impacts the surface, secondary electrons and ions are ejected

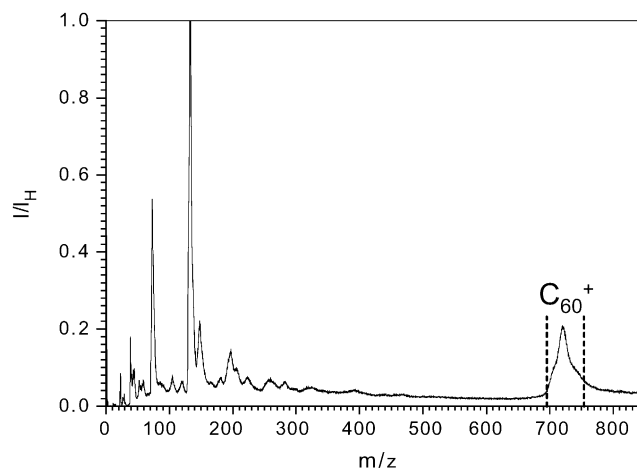


Fig. 2. Primary ion spectrum of C_{60} caused by ^{252}Cf fission fragments (dashed lines identify the primary ion window).

and accelerated through a second $\sim 48\text{ cm}$ ToF region. The secondary electrons are steered to a second MCP assembly by a weak magnetic field (<150 gauss) to signal the impact of a PI. Finally, any secondary ions produced by a PI impact are detected on a third MCP assembly.

All measurements are made in the event-by-event bombardment and detection mode described in detail elsewhere [4]. In brief, operating at low PI fluence ($<1000\text{ Hz}$), all PIs made by a FF on the source foil impact the sample surface at different times based on the m/z of the PI. For example, a FF produces a C_{60} ion and the complementary FF starts the electronics. Secondary electrons signal (Stop 1) the arrival of C_{60} at the sample target as well as the beginning of the secondary ToF stage. Any SIs originating from the impact are detected (Stop 2). In instances where both secondary electrons and ions are detected from an impact a SI spectrum can be made. This spectrum is the sum of all PI impacts and recorded secondary particles (Fig. 2). To look at secondary particles produced only by C_{60} , a window is set around the C_{60} peak in the PI spectra yielding a SI spectrum. The SI spectrum is convoluted because of the impact angle coupled with a large impact area ($\sim 2\text{ cm}^2$) which produces a time aberration in the arrival time of C_{60} . A software function compensates for the time aberration by electronically shifting the arrival times of the PIs in a selected window to the first channel in the window. The SIs associated with each PI event are shifted an equal number of channels yielding a SI mass spectrum (Fig. 3). Coincidental (co-emitted) ions are observed by setting a window around an ion of interest in the SI spectrum (Fig. 4).

2.2. Source foil and target preparation

Primary ion source materials were obtained from Sigma–Aldrich. Coronene and C_{60} were vapor deposited on mylar foil. One hundred microliters each of saturated solutions of gramicidin S and 3, 5-dimethoxy-4-hydroxy-

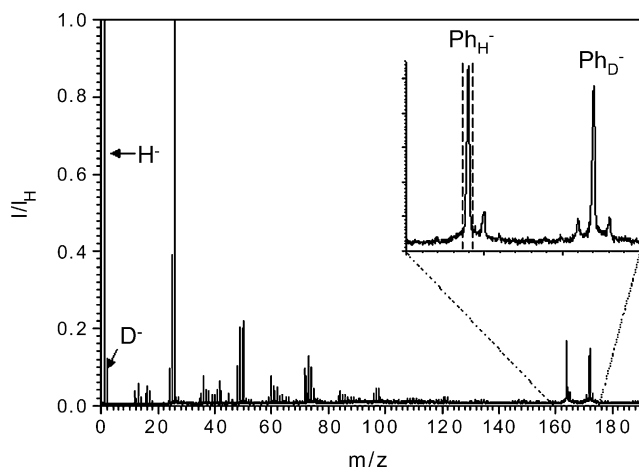


Fig. 3. Secondary ion spectrum produced by 21 keV C_{60} bombardment. The inset is an enlarged view of the molecular ion region (dashed lines identify the coincidental ion window).

cinnamic acid in methanol were mixed. Forty microliters of the mixture was deposited on a mylar foil and dried leaving a thin deposit of analyte and matrix. The target material was prepared by mixing equa-molar amounts of phenylalanine and deuterated-phenylalanine. The phenylalanine mixture was then vapor deposited on a stainless steel substrate.

2.3. Detection of multiple molecular ions

The secondary ions are monitored by linear ToF-MS. The ToF instrument uses a pulse counting arrangement and thus cannot report ion multiplicity (i.e., two or more ions of the same mass arriving simultaneously at the detector). To recognize the ejection of two molecular ions, we chose a target that consisted of an equimolar mixture of Ph (phenylalanine, Ph_H , $C_9H_{11}NO_2$, M_w 165.19) and deuterated Ph (deuterated-phenylalanine, Ph_D , $C_9H_3D_8NO_2$, M_w 173.26). This allows

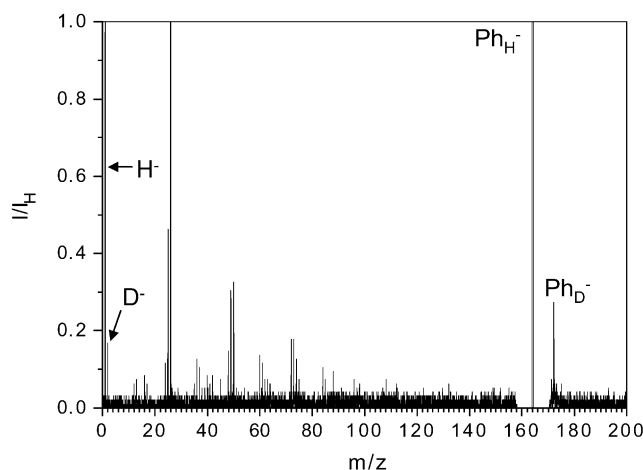


Fig. 4. Coincidental ion spectrum (all ions co-emitted with $164\ m/z$) produced by 21 keV C_{60} bombardment.

the detection of two phenylalanine molecular $[M-H]^-$ ions, Ph_H ($m/z = 164$) and Ph_D ($m/z = 172$), possessing similar physical characteristics [2].

3. Results and discussion

3.1. Secondary ion yields

The experimental secondary ion yields are influenced by the nature of the target surface. The following equations describe the experimental ion yield for a specific case (i.e., a surface composed of one-half Ph_H and one-half Ph_D)

$$Y(Ph)_{\text{exp}} = Y(Ph_H)_{\text{exp}} + Y(Ph_D)_{\text{exp}} = \frac{I(Ph_H)}{N} + \frac{I(Ph_D)}{N} \quad (1)$$

where $Y(Ph)_{\text{exp}}$ is the experimental ion yield of all $[M-H]^-$ phenylalanine ions, $Y(Ph_n)_{\text{exp}}$ is the experimental ion yield for $[M-H]^-$ phenylalanine ions of a specific fraction ($n = H$ or D), I is the number of detected ions of a specific target fraction, and N is the number of primary ion impacts. Each species represents 50% of the surface ($\rho = 0.5$), therefore

$$Y(Ph_H)_{\text{exp}} = Y(Ph_D)_{\text{exp}} \quad (2)$$

and

$$Y(Ph)_{\text{exp}} = Y(Ph_D)_{\text{exp}}/\rho \quad (3)$$

where ρ is the relative concentration.

The impact velocities of these projectiles are considerably different at identical impact energies. For example at 21 keV, the impact velocities of coronene, C_{60} , and gramicidin S are approximately 116.1 km/s, 75.0 km/s, and 59.6 km/s, respectively. In order to compare the projectiles at equal impact energies per constituent atom (neglecting hydrogen), the impact energies are divided by the atomic mass of the respective projectile. The SI yield is divided by atomic mass to compare the SI yields per constituent of the projectiles.

The yields of Ph are approximately the same for coronene and C_{60} projectiles at equal velocities. There is a linear relationship between the yield and the energy per projectiles atom (Fig. 5a and b). A similar trend was previously observed while bombarding an organic surface with carbon clusters having a few hundred eV per atom [10,13]. This behavior is in contrast to what is observed in bombardment with atomic ion and small cluster with kinetic energies of thousands of eV where the sputtering yield depends on the elastic stopping power. The present case of massive projectiles with impact energies of hundreds of eV per atom has been modeled by Bitensky and coworkers [14,15]. In this model, the dependence of the yield (Y^-) versus energy (E) for negatively charged secondary ions is expressed as follows:

$$Y^- \propto E \cdot f(x) \quad (4)$$

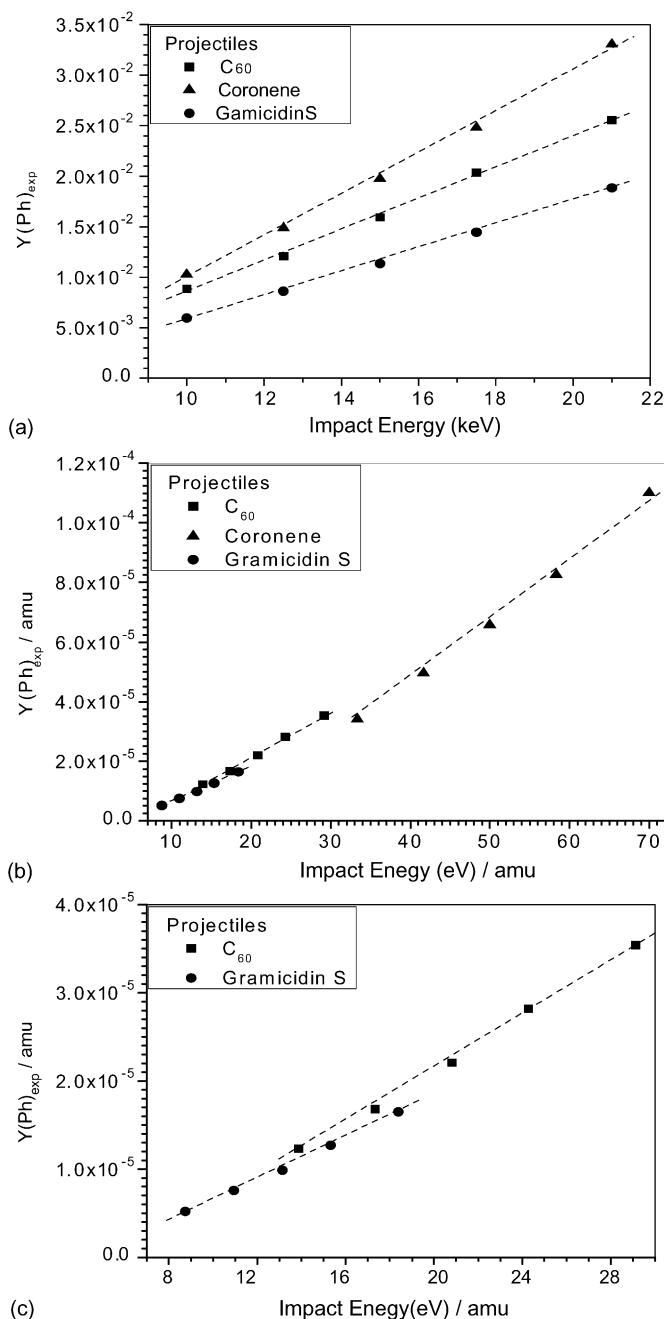


Fig. 5. (a) Secondary ion yields of Ph per projectile impact as a function of impact energy, (b) secondary ion yield per amu of Ph as a function of impact velocity, (c) enlarged view of the secondary ion yield per amu of Ph as a function of impact velocity (note: the SI yields of Ph are the sum of peak areas of PhH^- and PhD^-). The error bars for the data are $\pm 5\%$ (dashed lines are to guide the eyes).

where $f(x)$ is a complex power function [16]. The variable x is a function of the following parameters

$$x = \beta \cdot E^{1/3} / \exp\left(\frac{-z}{\lambda}\right) \quad (5)$$

where β is a projectile shape factor, which is highest for spherical projectiles; z is the ion formation depth inside the crater

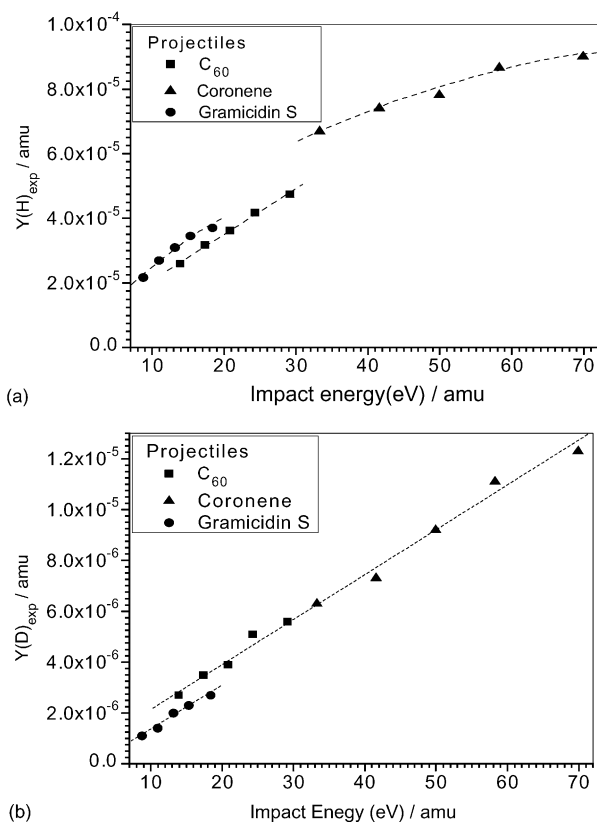


Fig. 6. (a) Secondary ion yield per amu of H^- as a function of projectile impact velocity, (b) secondary ion yield per amu of D^- as a function of projectile impact velocity (dashed lines are to guide the eyes).

created by the projectile, and λ is the mean free path of the secondary ion before neutralization. In the case of a high survival probability for the secondary ion ($x \ll 1$), the ions are emitted from the total crater volume and the expression (4) reduces to

$$Y^- \propto E \quad (6)$$

The experimental ion yield dependences reported here are well approximated by (6) within the experimental energy range (Figs. 5b, 6b). The dependences (4) and (6) are valid at impact conditions where crater formation occurs. It is probable in our case, that the Ph molecular ion has a high survival probability and is emitted from the entire volume of the crater. Our explanation fits with recent molecular dynamics simulations, which shows cluster emission from the entire volume of the craters perturbed by low energy C_{60} impacts [11].

The comparison of SI yields of H and D per constituent produced by equal velocity projectiles reveals several differences. The relative positions of D ion yields to the H ion yields from C_{60} and gramicidin S bombardment are inverted from one data set to the other. The SI yields of H from coronene and C_{60} impacts are not in alignment in the H data (Fig. 6a), while the SI yields of D from coronene and C_{60} are similar at equal velocity (Fig. 6b). This difference in the relative orientation of H and D secondary ion yields from C_{60} and

gramicidin S is directly related to the origin of the ions. The D ions must originate from the phenylalanine volume. However, hydrogen has three possible sources: the phenylalanine volume, surface contamination and the primary projectiles (coronene and gramicidin S). Recoiled hydrogen from gramicidin S increases the SI yield of H for this projectile which inverts the relative positions of the SI yields of D and H (i.e., for yields of H, gramicidin S has a higher yield than C_{60} while the yield of D is higher for C_{60} than gramicidin S at equal velocities). Similar observations of recoiled ions have been observed [17]. These additional hydrogen sources may account for the deviation of hydrogen yields (Fig. 6a) from the behavior described by Eq. (6).

The yields of Ph caused by C_{60} impacts is ~ 20 percent higher than the yields of Ph caused by gramicidin S impacts at equal velocities (Fig. 5c). This is also observed in the yields of deuterium (Fig. 6b). The primary projectile structure may influence the SI yields as explained by the Bitsensky model [14]. According to this model, one parameter affecting the sputtering yield is the projectile shape factor (β). The structural differences in the projectiles (i.e., C_{60} is a rigid, covalently bonded, sphere, while gramicidin S is a comparatively flexible, hydrogen-bonded, quasi-spherical structure) may influence the emission of secondary ions from C_{60} and gramicidin S impacts.

A second explanation for the higher yield produced by C_{60} compared to gramicidin S may be attributed to changes in the ionization process because of the direct deposition of oxygen into the desorption volume. It is well documented that many factors, such as surface work function, ionization potential and electron affinity of the emitted ions affects the ionization probability. The important of each factor varies depending on the ionization process [18]. Several studies have shown increases in the SI yields of both anions and cations from single crystal surfaces in the presence of oxygen [19–21]. More relevant to our experiment are observations made involving carbide surfaces. It was observed that oxygen absorption decreased the emission of most carbon containing ions on carbide surfaces [22]. The depression of D and Ph yields produced by gramicidin S may be attributed to changes in the ionization process because of the presence of oxygen in gramicidin S (Figs. 5b, 6b).

3.2. Coincidental ion yields

The coincidental (co-emitted) ion yields are also influenced by the nature of the target surface. The following equations describe the experimental ion yield for a specific case (i.e., a surface composed of one-half Ph_H and one-half Ph_D)

$$Y(Ph_H, Ph_D)_{\text{exp}} = \frac{I(Ph_H, Ph_D)}{N} \quad (7)$$

where $Y(Ph_H, Ph_D)_{\text{exp}}$ is the ion yield of Ph_D co-emitted with Ph_H , $I(Ph_H, Ph_D)$ is the measured number of events when Ph_D co-emitted with Ph_H , and N is the number of primary ion impacts. The coincidental yield corresponds to a mixed

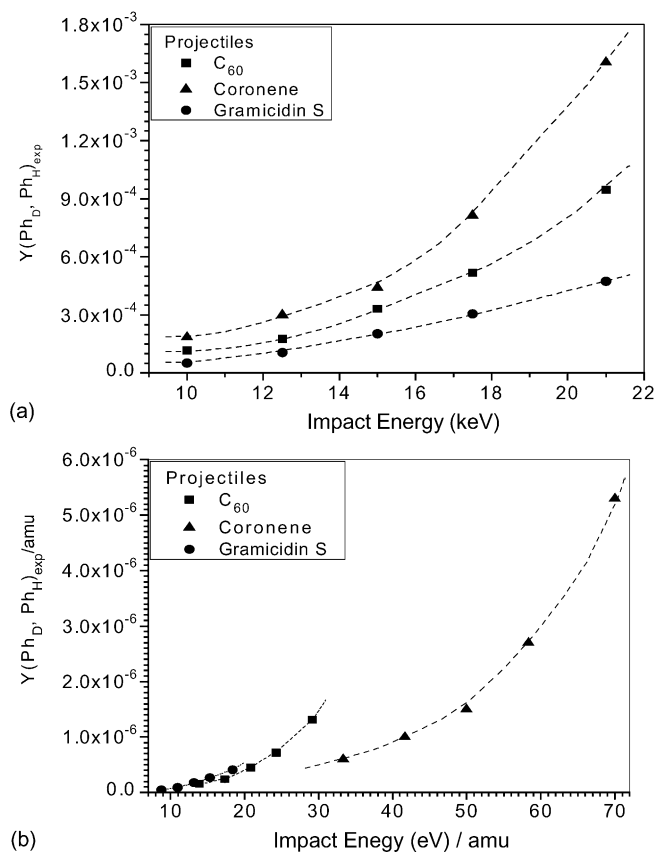


Fig. 7. (a) Experimental secondary ion yields of two co-emitted Ph ions per projectile impact as a function of impact energy, (b) experimental secondary ion yields of two co-emitted Ph ions per amu as a function of projectile impact velocity. The error for the data varies between $\pm 12\%$ at 10 keV impact energy to $\pm 5\%$ at 21 keV impact energy (dashed lines are to guide the eyes).

Ph target surface ($\rho = 0.5$), therefore

$$Y(Ph, Ph)_{\text{exp}} = Y(Ph_H, Ph_D)_{\text{exp}}/\rho^2 \quad (8)$$

where $Y(Ph, Ph)_{\text{exp}}$ is the experimental yield of two co-emitted Ph molecules, $Y(Ph_H, Ph_D)_{\text{exp}}$ is the measured yield of two co-emitted Ph molecules, and ρ is the relative concentration.

Fig. 7a shows the yield of Ph_D co-emitted (coincidental) with Ph_H from coronene, C_{60} and gramicidin S versus impact energy. The yield for co-emitted ions and impact energy are divided by the atomic mass of the respective projectiles (neglecting hydrogen) for reasons previously mentioned. The coincidental ion (CI) yields per constituent for C_{60} and gramicidin S are comparable at the impact energies examined (Fig. 7b).

In contrast to the linear dependence $Y(Ph)_{\text{exp}}$ versus energy for single Ph ion emission, the dependence $Y(Ph, Ph)_{\text{exp}}$ versus energy for two Ph ions emissions is nonlinear. Significant differences in projectile efficiencies emerge when comparing the CI yields of coronene and C_{60} . The trend for C_{60} suggests that at equal velocities this projectile is

intrinsically more effective for the co-emission of two Ph ions than coronene. This evidence supports a collective collision cascade mechanism, which has been examined with molecular dynamics (MD) simulations. MD simulations examining keV C₆₀ sputtering have shown that the impacts produce multiple overlapping cascades in a relatively shallow volume resulting in the emission of many particles [11].

4. Conclusions

We report here the first experimental data for coincidental ion emission by these types of carbon containing projectiles. The key observation is the supralinearity of the yield of co-emitted phenylalanine ions versus the kinetic energy of the projectile. The results demonstrate that C₆₀ is a promising projectile for organic surface analysis as well as for the production of multi-ion emission. Further examination of the behavior of the yield of co-emitted phenylalanine ions versus kinetic energy of the projectile, needs a data acquisition scheme where multi-ion emission processes (i.e., emission of 3, 4, . . . ions) can be measured.

This research was supported by the NSF (CHE-0135888) and R.A. Welch Foundation (A-1482).

References

- [1] M.G. Blain, S. Della-Negra, H. Joret, Y. Le Beyec, E.A. Schweikert, *Phys. Rev. Lett.* 63 (1989) 1625.
- [2] R.D. Rickman, S.V. Verkhoturov, E.S. Parilis, E.A. Schweikert, *Phys. Rev. Lett.* 92 (2004) 47601.
- [3] S. Bouneau, A. Brunelle, S. Della-Negra, J. Depauw, D. Jacquet, Y. Le Beyec, M. Pautrat, M. Fallavier, J.C. Poizat, H.H. Anderson, *Phys. Rev. B* 65 (2002) 144106.
- [4] M.J. Van Stipdonk, R.D. Harris, E.A. Schweikert, *Rapid Com. Mass Spectrom.* 10 (1996) 1987, and references therein.
- [5] D. Weibel, S. Wong, N. Lockyer, P. Blenkinsopp, R. Hill, J.C. Vickerman, *Anal. Chem.* 75 (2003) 1754.
- [6] G. Gillen, L. King, B. Freibaum, R. Lareau, J. Bennett, F. Chmara, *J. Vac. Sci. Technol. A* 19 (2000) 568.
- [7] A.D. Appelhans, J.E. Delmore, *Anal. Chem.* 61 (1989) 1087.
- [8] D. Stapel, M. Thiemann, A. Benninghoven, *Appl. Surf. Sci.* 158 (2000) 362.
- [9] J. Xu, C.W. Szakal, S.E. Martin, B.R. Peterson, A. Wucher, N. Winograd, *JACS* 126 (2004) 3902.
- [10] M. Benguerba, A. Brunelle, S. Della-Negra, J. Depauw, H. Joret, Y. Le Beyec, M.G. Blain, E.A. Schweikert, G. Ben Assayag, P. Sudraud, *Nucl. Instrum. Meth. B* 62 (1991) 8.
- [11] Z. Postawa, B. Czerwinski, M. Szewczyk, E.J. Smiley, N. Winograd, B.J. Garrison, *J. Phys. Chem. B* 108 (2004) 7831.
- [12] S.V. Verkhoturov, E.A. Schweikert, N.M. Rizkalla, *Langmuir* 18 (2002) 8836.
- [13] K. Boussofiene-Baudin, G. Bolbach, A. Brunelle, S. Della-Negra, P. Hakansson, Y. Le Beyec, *Nucl. Instrum. Meth. B* 88 (1994) 160.
- [14] I.S. Bitensky, D.F. Barofsky, *Phys. Rev. B* 56 (1997) 13815, and references therein.
- [15] P. Sigmund, I.S. Bitensky, J. Jenson, *Nucl. Instrum. Meth. B* 112 (1996) 1.
- [16] R.A. Zubarev, I.S. Bitensky, P.A. Demirev, B.U.R. Sundqvist, *Nucl. Instrum. Meth. B* 88 (1994) 143.
- [17] C.W. Diehnelt, M.J. Van Stipdonk, E.A. Schweikert, *Nucl. Instrum. Meth. B* 142 (1998) 606.
- [18] L. Hanley, O. Kornienko, E.T. Ada, E. Fuoco, J.L. Trevor, *J. Mass Spectrom.* 34 (1999) 705.
- [19] P. Williams, C.A. Evans Jr., *Surf. Sci.* 78 (1978) 324.
- [20] K. Wittmack, *Surf. Sci.* 112 (1981) 168.
- [21] H. Gnaser, *Surf. Sci.* 138 (1984) 561.
- [22] A. Benninghoven, F. Rudenauer, H. Werner, *Secondary Ion Mass Spectrometry*, Wiley & Sons, New York, 1987, p. 229.